BeppoSAX Observations of the Maser Sy2 Galaxy: ESO103-G35.

Belinda J. Wilkes[1], Smita Mathur,[1,2]Fabrizio Fiore,[3,4] Angelo Antonelli,[3,4] & Fabrizio Nicastro[1]

1: Harvard-Smithsonian Center for Astrophysics, Cambridge, MA 02138

2: The Ohio State University

3: BeppoSAX Science Data Center, via Corcolle 19, I-00131, Roma, Italy

4: Osservatorio Astronomico di Roma, via Frascati 33, I-00040 Monteporzio, Italy

Received _____; accepted _____

To appear in ApJ

ABSTRACT

We have made BeppoSAX observations of the Seyfert 2/1.9 galaxy ESO103-G35, which contains a nuclear maser source and is known to be heavily absorbed in the X-rays. Analysis of the X-ray spectra observed by SAX in October 1996 and 1997 yields a spectral index $\alpha_E = 0.74 \pm 0.07$ ($F_\nu \propto \nu^{-\alpha_E}$) which is typical of Seyfert galaxies and consistent with earlier observations of this source. The strong, soft X-ray absorption has a column density, N_H of $1.79 \pm 0.09 \times 10^{23}$ cm^{-2}, again consistent with earlier results. The best fitting spectrum is that of a power law with a high energy cutoff at 29±10 keV, a cold (E=6.3±0.1 keV, rest frame), marginally resolved ($\sigma = 0.35 \pm 0.14$ keV, FWHM $\sim 31 \pm 12 \times 10^3$ km s^{-1}) Fe Kα line with EW 290^{+100}_{-80} eV (1996) and a mildly ionized Fe K-edge at $7.37^{+0.15}_{-0.21}$ keV, $\tau = 0.24^{+0.06}_{-0.09}$. The K$\alpha$ line and cold absorption are consistent with origin in a accretion disk/torus through which our line-of-sight passes at a radial distance of $\sim$ 50 pc. The Fe K-edge is mildly ionized suggesting the presence of ionized gas probably in the inner accretion disk, close to the central source or in a separate warm absorber. The data quality is too low to distinguish between these possibilities but the edge-on geometry implied by the water maser emission favors the former. Comparison with earlier observations of ESO103-G35 shows little/no change in spectral parameters while the flux changes by factors of a few on timescales of a few months. The 2–10 keV flux decreased by a factor of $\sim$ 2.7 between Oct 1996 and Oct 1997 with no detectable change in the count rate >20 keV (i.e. the PDS data). Spectral fits to the combined datasets indicate either a significant hardening of the spectrum ($\alpha_E \sim 0.5$) or a ∼constant or delayed response reflection component. The high energy cutoff (29±10 keV) is lower than the typical $\sim$ 300 keV values seen in Seyfert galaxies. A significant subset of similar sources would affect current

models of the AGN contribution to the cosmic X-ray background (CXRB) which generally assume a high energy cutoff of ~ 300 keV.

Subject headings: X-ray, AGN, masers, CXRB

1. Introduction

The sub-parsec masing disk recently found to be orbiting a $\sim 10^7$ solar mass black hole in the Seyfert 2 galaxy, NGC 4258, provides the most compelling evidence to date for the existence of a massive black hole in the nucleus of a galaxy (Miyoshi *et al.* 1995). The disk is edge-on, the X-ray spectrum is heavily absorbed (Makishima *et al.* 1995) and an active nucleus is visible in polarized light (Wilkes *et al.* 1995). Nearly all AGNs which contain maser sources and have X-ray observations show strong X-ray absorption consistent with an edge-on disk, suggesting that they generally harbor active nuclei in their cores. This is consistent with the generally accepted scenario that many Seyfert 2 galaxies are edge-on Seyfert 1 galaxies (Antonucci & Miller 1985). The combined power of the high-resolution radio observations and the X-ray spectrum to study the structure of the disk both along the line-of-sight and in the plane of the sky makes these objects potentially key to our understanding of the inner regions of active galaxies.

The Seyfert 1.9/2 galaxy ESO103-G35 is a strong X-ray source, originally discovered by HEAO 1/A2 (H1834-653, Marshall *et al.* 1979, Piccinotti *et al.* 1982). It was identified as a Seyfert 1.9 galaxy at a redshift of 0.0133 by Phillips *et al.* (1979) though later spectra have shown no evidence for broad lines (Morris & Ward 1988) leaving its classification in some doubt. It has been observed extensively in the X-rays. EXOSAT observations revealed strong, soft X-ray absorption ($N_H \sim 2 \times 10^{23}$ cm-2) which showed a factor of 2 variation over 90 days (Warwick, Pounds & Turner 1988), providing some of the first evidence for variable absorption in a Seyfert nucleus. *Ginga* observations revealed an equivalent width $\sim$ 330 eV Fe Kα emission line whose origin was not clear given the presumed (but not confirmed) presence of a flaring source within the *Ginga* beam during a portion of this observation (Warwick *et al.* 1993). The continuum spectrum was consistent with that reported by EXOSAT.

ASCA observations confirmed and extended the earlier studies, reporting a cold, resolved Fe Kα emission line and a mildly ionized Fe K-edge (Turner *et al.* 1997, Forster, Leighly & Kay 1999). While flux variations up to a factor of a few are common on short timescales, no significant spectral or absorption variations have been detected.

Recent radio measurements have revealed water maser emission in the form of a single line at +100 km s^{-1} (Braatz, Wilson & Henkel 1997) with respect to the AGN redshift. Due to the large negative declination ($\delta \sim -65^o$) of this source, higher resolution and sensitivity observations to further study this maser are difficult at present. However the combination of water maser emission and the strong, absorbed X-ray source suggest a strong parallel with NGC4258 and motivated our observations with BeppoSAX to obtain an X-ray spectrum simultaneously over a wide energy band (1–200 keV). The moderate spatial resolution ($\sim 2'$) of BeppoSAX facilitates identification of any nearby, contaminating sources and so avoids the confusion present in the *Ginga* data. Here we present an analysis of the BeppoSAX X-ray data.

2. Observations and Analysis.

ESO103-G35 was observed with BeppoSAX at two epochs: Oct 1996 and Oct 1997 (see Table 1). Data were obtained with both gas scintillator proportional counter (GSPC) detectors: low and medium energy concentrator spectrometers (LECS and MECS respectively, Parmar *et al.* 1990) and with the Phoswich detector system (PDS, Frontera *et al.* 1991). The source was clearly detected and unresolved in all three detectors and no nearby source of comparable strength was seen.

Counts were extracted from a $4'$ circle in both LECS and MECS detectors and background counts subtracted, estimated from the background file appropriate for this

extraction radius provided by the BeppoSAX Data Center (SDC) as of March 1998. The resulting net source count rates for the energy ranges over which the instrument calibration is reliable are listed in Table 1. The PDS data were background subtracted as part of the data reduction pipeline.

Table 1: Observational details for the BeppoSAX observation of ESO103-G35.

Start Date	End Date	Instrument	Exp. Time (ksecs)	Energies (keV)	Count Rate (cts s^{-1})
3 Oct 1996	4 Oct 1996	LECS	10.238	0.1–5.0	0.031±0.002
		MECS	50.615	1.7–10.5	0.306±0.003
		PDS	21.029	15–200	0.75±0.04
14 Oct 1997	15 Oct 1997	MECS	14.312	1.7–10.5	0.122±0.003
		PDS	5.9	15–200	0.73±0.11

The spectra were analyzed with the XSPEC spectral fitting package (Arnaud 1996) using the calibration files provided by the SDC (March 1998). The data from all three instruments were fitted simultaneously. Following the recommendation of the SDC, we constrained the PDS normalization to be 0.85 times that of the MECS. We first fitted the data with an absorbed power-law model (Table 2, fit 1). The best fit value of the column density (z=0) $N_H = (2.07 \pm 0.007) \times 10^{23}$ cm^{-2} is significantly larger than the Galactic column density towards the source ($N_H \lesssim 3 \times 10^{20}$ cm^{-2}). The absorbed power law fit showed a clear excess in both datasets at the position of the Fe Kα emission line ($\sim$ 6.4 keV). Addition of a Gaussian emission line resulted in an acceptable fit (Table 2, fit 2, Figure 1) with a χ^2_ν of 1.16 (239 degrees of freedom, dof). The emission line equivalent width (EW) is $=240^{+80}_{-60}$ eV and it is marginally resolved. However the residuals at high energies show an excess suggestive of curvature. We therefore applied first a high energy cutoff to the powerlaw (Table 2, fit 3) and then a reflected component with no high energy

cutoff (Table 2, fit 4). The former resulted in a significantly improved χ^2_ν (f-test yields 0.01% significance level). The results are displayed in Figures 2 and 3 respectively.

The 1996 ASCA data (Turner *et al.* 1997, Forster *et al.* 1999) showed an iron edge at about $7.37^{+0.26}_{-0.22}$ keV with $\tau = 0.47^{+0.16}_{-0.12}$, consistent with earlier observations (Warwick *et al.* 1993). Since systematic residuals are present around 7–8 keV in the best fit spectrum (Figure 2), we investigated the presence of excess iron absorption. We added an edge to the best fit model described above and indeed found an $> 99\%$ improvement in the fit (F-test). The best fit edge energy is $7.37^{+0.15}_{-0.21}$ keV, consistent with ASCA observations in March 1996 (Forster *et al.* 1999), with an opacity, $\tau = 0.24^{+0.06}_{-0.09}$, marginally ($\sim 2\sigma$) lower than the ASCA value. This absorption is likely due to the K-edge of mildly ionized iron. However, our data quality is not good enough to fit a complex warm absorber model. We tried using the 'absorbi' model in XSPEC, but could not constrain the parameters.

The 1997 dataset has a lower MECS count rate and shorter exposure time so that the data have much lower signal-to-noise (see Table 1, Figure 4). To quantify the amount of variation, we first fitted a simple absorbed power law plus Gaussian emission line model to the MECS data only. The results are given as fit 5 in Table 3 and displayed in Figure 4. The flux decreased by a factor of ~ 2.7 over the year between the two observations. There is no evidence for spectral variability or for a variable absorbing column density. The emission line strength is poorly constrained, EW=250^{+150}_{-110} eV, and is consistent with either a constant flux or constant EW over the year. We therefore are unable to constrain the response time of the line-emitting material to the continuum variations. There is no evidence in this spectrum for the line to be broad, though once again the errors are sufficiently large that it remains consistent with the 1996 line width.

Surprisingly, the PDS data in the 1997 dataset show a count rate similar to the 1996 value (Table 1). We fitted the combined MECS+PDS data for 1997. An absorbed power

law plus Gaussian line fit to the combined dataset shows a flatter slope (see Table 3, fit 6) and gives an acceptable χ^2 value. The resulting spectral index ($\alpha_E \sim 0.5$) is much flatter than in 1996 and would imply a significant hardening of the spectrum as the flux decreases. Since there is no other evidence for spectral variability in ESO103-G35, we seek an alternative interpretation.

Partial covering of a hard continuum source can be ruled out by the lack of variability in the PDS data. However, since the PDS data would be dominated by any reflected component, an alternative interpretation of this pattern of variability is that of a reflected component which remains constant while the power law component varies. Fit 7 (Table 3) shows the best fitting power law plus reflection plus Gaussian line model to the MECS+PDS 1997 dataset. This gives a marginally better fit but the data are not of sufficiently high quality to provide strong contraints on the parameters. For this to be realistic, the reflecting medium must respond to a change in incident continuum with some delay or be seeing a constant continuum which is invisible to us. This latter could occur, for example, if the flux variation were due to absorption by material between us and the reflecting material. However the spectrum shows no evidence for a variation in the column density to support this scenario. The most likely explanation is that of a reflected component, undetectable in the earlier dataset and with a delayed response to continuum variations. With only two data points, we cannot be sure whether further continuum variations occurred during the period in between our observations to which the reflected component is responding. Thus we cannot place any meaningful constraints on the distance of the reflecting region from the continuum source.

3. Discussion

3.1. Absorption

The BeppoSAX observations confirm the presence of a large column density of neutral absorbing material ($N_H = 2.0 \pm 0.1 \times 10^{23}$ cm^{-2}) in the X-ray spectrum of ESO103-G35. The column density measured here is consistent with the higher column density reported in the EXOSAT data (Warwick *et al.* 1988) as well as that from more recent ASCA data (Forster *et al.* 1999, Turner *et al.* 1997). There is no evidence for variation in this absorbing column between the 1996 and 1997 observations. Figure 5 and Table 4 show a compilation of N_H measurements over a 13 year period (1984−1997). They are generally consistent with one another, the largest deviation[1] is $\sim 2\sigma$ in 1991.

Absorbing material with column densities $\sim 10^{23}$ cm^{-2} is typically seen in the subset of Seyfert 2 galaxies which show evidence for a hidden Seyfert 1 (Turner *et al.* 1997, Awaki 1997). It is consistent with a line-of-sight passing through an edge-on, optically thick accretion disk/torus of neutral material such as is commonly believed to be present in Seyfert galaxies (Antonucci & Miller 1985). The presence of water maser emission in ESO103-G35 (Braatz *et al.* 1997) indicates that our line-of-sight intersects the accretion disk/torus accurately edge-on. In the absence of warps in the disk/torus, the X-ray absorption measures its full column density.

We also detect excess absorption due to ionized iron, most likely due to FeII–FeXV, consistent with earlier Ginga and ASCA results. The observed opacity $\tau = 0.24^{+0.06}_{-0.09}$ is somewhat lower than the ASCA value (Turner *et al.* 1997, Forster *et al.* 1999). While our data quality are insufficient to constrain a full warm absorber model, the presence of

[1]apart from the rapid change reported by Warwick *et al.* (1988) which may have been due to a spurious source in the *Ginga* data (§1)

the edge requires ionized material along our line-of-sight. Given the accurately edge-on geometry, the ionized material most likely lies within the inner regions of the accretion disk/torus close to the central continuum source. One possible alternative would be a warp in the disk/torus so that our line-of-sight does not pass through the full geometric size of the disk. A sufficiently strong warp would allow the possibility of a separate warm absorber above or below the accretion disk/torus at a position closer to the central source than the intersection of the warped disk with our line-of-sight.

3.2. Spectral Shape

The best fitting model is a cutoff power law with slope, $\alpha_E = 0.74 \pm 0.07$ (Table 2, fit 3), a cutoff with energy of 29±10 keV and e-folding energy 40^{+30}_{-20}keV. This model shows a resolved Fe Kα emission line at 6.3±0.1 keV and equivalent width 290^{+100}_{-80} eV. Figure 5 shows the lack of significant variation in spectral parameters over a 13 year period.

In the hard X-ray, where the effects of the large absorbing column are negligible, the scenario of Seyfert 2 galaxies being edge-on Seyfert 1s predicts that both classes of galaxy look similar. Hard X-ray and γ-ray data for radio-quiet Seyfert 1 galaxies typically show a power law spectrum with spectral index, $\alpha_E \sim 0.9$, similar to that reported here for ESO103-G35 but extending to energies > 100 keV (Gondek *et al.* 1996) rather than ~ 30 keV. This hard X-ray spectrum can be explained by emission from an optically thin, relativistic, thermal plasma in a disk corona or by a non-thermal plasma with a power-law injection of relativistic electrons (Gondek *et al.* 1996). The lower high energy cutoff suggests this component has a higher optical depth in ESO103-G35. In addition the X-ray spectra of radio-quiet Seyfert 1 galaxies typically include a contribution from Compton reflection in warm material which is superposed on the underlying power law in the energy range 10–100 keV (Gondek *et al.* 1996). The 1996 observation favors a cutoff power law over a

reflection model suggesting that this latter component is, at most, weak in ESO103-G35 in its brighter state. However the relatively strong hard flux in the otherwise lower luminosity 1997 dataset suggests the presence of a reflection component in 1997. Since the reflection model includes a large number of parameters, it is not possible to constrain them usefully. However if we assume an isotropic source situated above the accretion disk, no high energy cutoff and solar abundances we deduce an inclination angle for the disk in the range $50^\circ - 90^\circ$, consistent with ESO103-G35 being a Sy1.9/2 in unified models and with the accurately edge-on geometry implied by the presence of water maser emission.

3.3. Luminosity Variation

Figure 5 shows the historical light curve of ESO103-G35 since 1983 including the current BeppoSAX observations (1997). It is clear that flux variations of factors of a few are common on timescales of months. The variation seen by ASCA and BeppoSAX between 1994 and 1997 shows a slow rise and rapid fall quite similar to that seen by *Ginga* between 1983 and 1985. The flux level in the 1996 observation (F(2–10 keV) = $2.57\pm0.07\times10^{-11}$ erg cm^{-2} s^{-1}) indicates a luminosity, $L_x \sim 2 \times 10^{43}$ erg s^{-1} (H_0=50, q_0=0).

3.4. Fe Kα Emission Line

The emission line is cold (6.3±0.1 keV), but consistent with being mildly warm, and marginally resolved (Table 2). Adopting an MECS instrument energy resolution of (σ) 0.21 keV at 6.3 keV (SAX Observers' Handbook), the intrinsic width of the line is estimated to be 0.28±0.12 keV which yields a FWHM of $\sim (31 \pm 12) \times 10^3$ km s^{-1} for the Fe Kα line. This indicates an origin in neutral, high-velocity material. The EW, 290^{+100}_{-80} eV, is within the wide range of observed values for Seyfert 2 galaxies and is consistent with fluorescence

in the cold absorber, the accretion disk/torus, which is attenuating the observed X-ray continuum (Awaki *et al.* 1991, Turner *et al.* 1997).

The emission line in the second dataset is not well-constrained. It is consistent with constant flux or with constant equivalent width over the one year period so we cannot determine if any response to the continuum variation has occurred. From the $\sigma = 0.32$ keV (Table 2), the FWHM of the line is about 30,000 km s^{-1}.

If the line width is dynamic, indicating a virial velocity around the 10^7 M$_\odot$ black hole, then the radial distance to the emitter is about 50 pc. We note that an alternative interpretation of the broad Fe K-α line is that of a mix of neutral and ionized material. This would be consistent with the earlier suggestion (§3.1) of ionized material in the inner regions of the accretion disk/torus being responsible for the ionized Fe-K edge. Fits to the 1994 ASCA dataset with three narrow lines covering a range of ionization were statistically indistinguishable from those with a broadened, neutral line (Turner *et al.* 1997).

3.5. The High Energy Cutoff

BeppoSAX, with its high energy response, has provided information on the high energy spectrum of a number of AGN for the first time. The dispersion and errors in the observed values of high energy cutoff of AGN are high but values typically range from 100−400 keV (Matt 1998). The high energy spectrum of AGN is a critical parameter for matching both the turnover at $\sim$ 30 keV and the high energy source counts when modelling the CXRB. Successful models generally adopt a value of 300 keV and require strong evolution in the number of absorbed AGN with redshift (Gilli, Risaliti & Salvati 1999). However, the high energy cutoff determined from our BeppoSAX data for ESO103-G35 (29±10 keV) is significantly lower, calling into question the validity of the modelling to date. More realistic

modelling of the distribution of AGN spectral properties, including the high energy cutoff, is required to make an accurate assessment of the AGN contribution to the CXRB (Yaqoob 2000).

4. Conclusions

ESO103-G35 is an X-ray bright, Sy 1.9/2.0 galaxy containing one of strongest water maser sources known implying that it is viewed accurately edge-on. The presence of cold molecular material along the line of sight to the active nucleus supports this picture. The amount of X-ray absorption has been ∼constant over the past 15 years and, at 2×10^{23} cm^{-2}, it is typical of Seyfert 2 galaxies and consistent with a line-of-sight passing through the edge-on accretion disk/torus also responsible for the maser emission.

We observe a marginally resolved Fe-Kα emission line whose width, if dynamic, implies a radial distance to the absorber of about 50 pc, similar to that expected for an obscuring torus. Alternatively, the width may be due to a range of ionization states in the emitting material consistent with the ionized Fe K edge at $7.37^{+0.15}_{-0.21}$ keV. The Fe Kα line strength (EW=290^{+100}_{-80} eV) and width are consistent with origin in an accretion disk/torus through which our line-of-sight is passing. The presence of both cold and warm (ionized) absorbing (and emitting) material suggests that the inner parts of the torus/disk are mildly ionized while the outer parts are cold.

The flux level in the energy range 0.6−10 keV decreased by a factor ~ 2.7 between October 1996 and October 1997 with no evidence for a change in spectral shape or absorption. However the 10-50 keV flux did not change between the two observations suggesting either a hardening of the hard continuum or the presence of a reflection component (undetectable at the higher flux level) which reacts to continuum changes with

some delay. Given the paucity of datapoints, we are unable to place meaningful constraints on the distance of the reflecting material from the continuum source.

The 1996 dataset shows a high energy cutoff at 29 ± 10 keV. This is significantly lower than the values ~ 300 keV believed typical to date (Gondek *et al.* 1996, Matt 1998). The high energy spectrum of AGN is critical for modelling the AGN contribution to the CXRB so that this result emphasizes the need to include a realistic distribution of cutoff energy in these models.

BJW and SM gratefully acknowledge the financial support of NASA grants: NAG5-7064 (BeppoSAX), NAG5-3249 (LTSA).

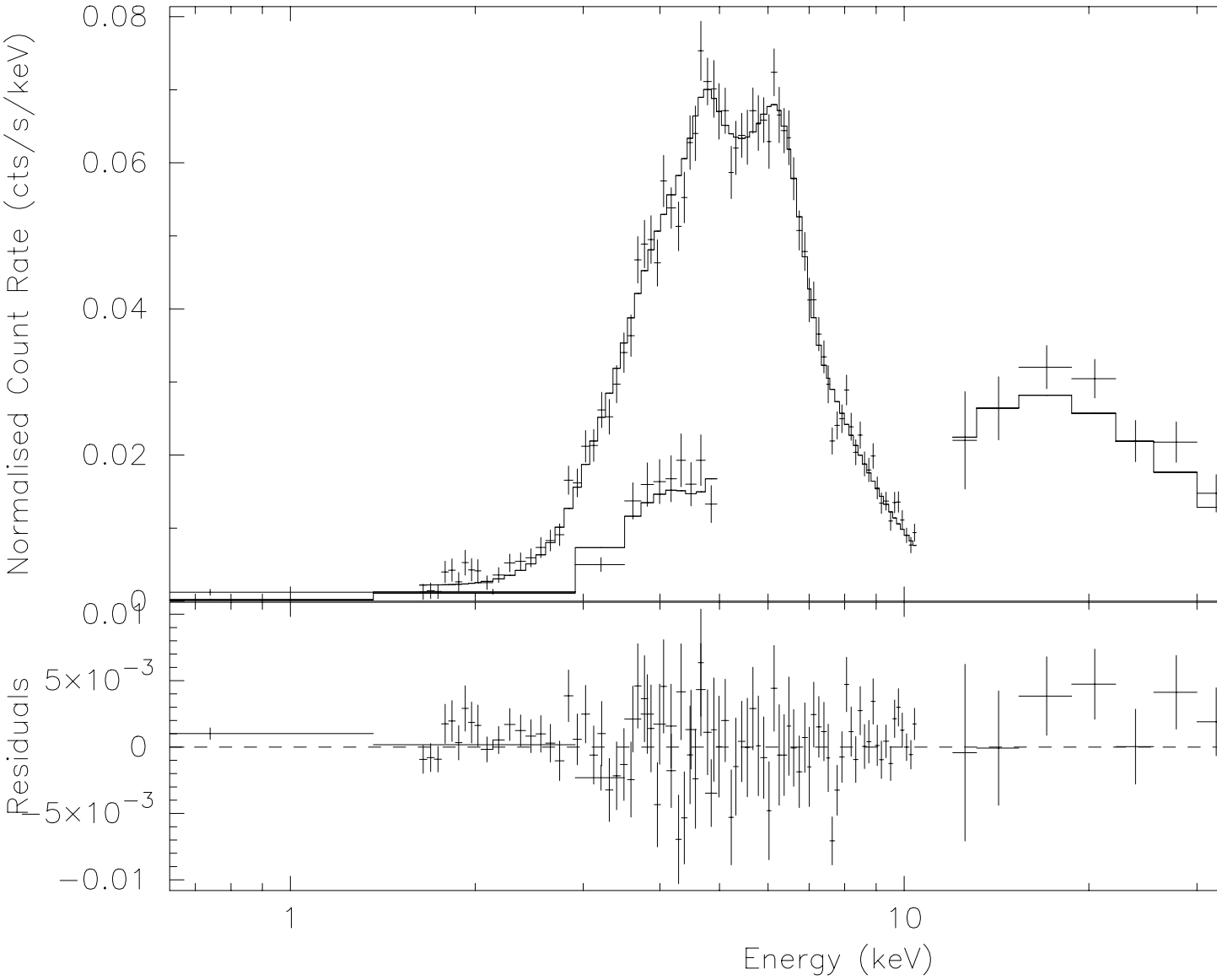

Fig. 1.— Best fitting power law plus gaussian emission line model for the epoch 1996 BeppoSAX data for ESO103-G35 over the energy range 0.6–100 keV (Table 2, Fit 2). The figure shows the data and best fit model folded through the instrument response with the residuals in the lower panel.

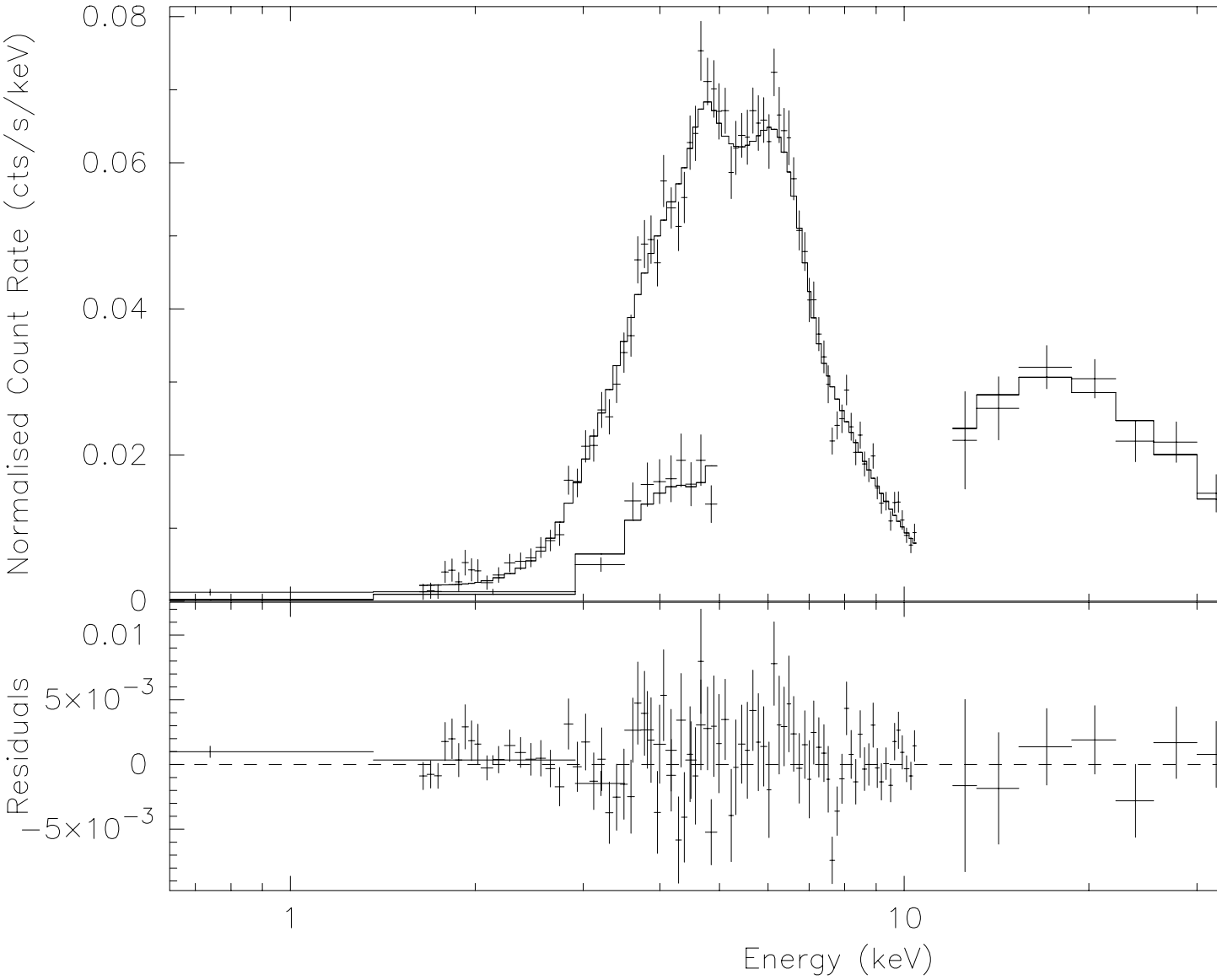

Fig. 2.— Best fitting cutoff power law plus gaussian emission line for the epoch 1996 BeppoSAX data of ESO103-G35 over the energy range 0.6–100 keV (Table 2, fit 3). The figure shows the data and best fit model folded through the instrument response with the residuals in the lower panel.

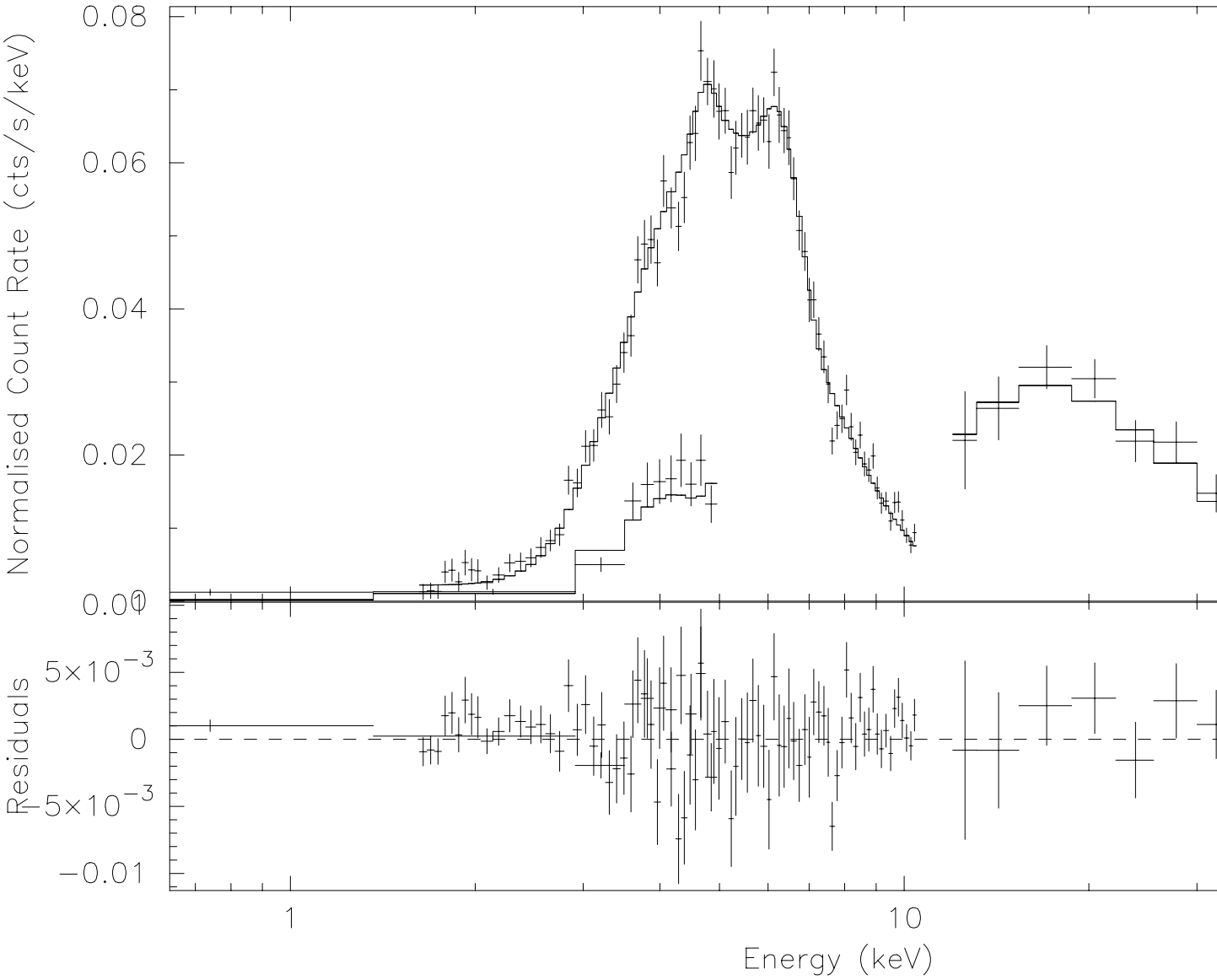

Fig. 3.— Best fitting power law plus gaussian emission line plus reflection model for the epoch 1996 BeppoSAX data of ESO103-G35 over the energy range 0.6–100 keV (Table 2, fit 4). The figure shows the data and best fit model folded through the instrument response with the residuals in the lower panel.

Table 2: Results of spectral fits to the 1996 dataset[1].

Fits	1	2	3	4
Model[2]	PL	PL+Gauss	PL+HighEcut+Gauss	PL+Refl+Gauss
N_H ($\times 10^{23}$cm^{-2})	2.07±0.07	1.92±0.08	1.79±0.09	1.97±0.09
F_ν(1 keV)[3]	0.024	0.019±0.003	0.015±0.002	0.024±0.005
α_E	0.94±0.05	0.87±0.05	0.74±0.07	1.00±0.12
Energy (keV)	-	6.33±0.10	6.30±0.10	6.34(fr)
σ (keV)	-	0.32± 0.14	0.35±0.14	0.30(fr)
EW(FeKα)(eV)	-	240^{+80}_{-60}	290^{+100}_{-80}	210^{+60}_{-40}
E_{cutoff} (keV)	-	-	29±10	-
E_{fold} (keV)	-	-	40^{+30}_{-20}	-
cos i (R=1)	-	-	-	$0.2^{+0.4}_{-0.2}$
χ^2_ν(dof)	2.05(103)	1.51(99)	1.28(96)	1.46(101)
Flux(2-10 keV)[4]	2.57	2.56	2.57	2.55

1: All errors are quoted at 90% confidence

2: PL: Power Law; Gauss: Gaussian emission line; HighEcut: a high energy exponential cutoff; Refl: reflection component

3: in photons cm^{-2} s^{-1} keV^{-1}

4: in units of 10^{-11} erg cm^{-2} s^{-1}

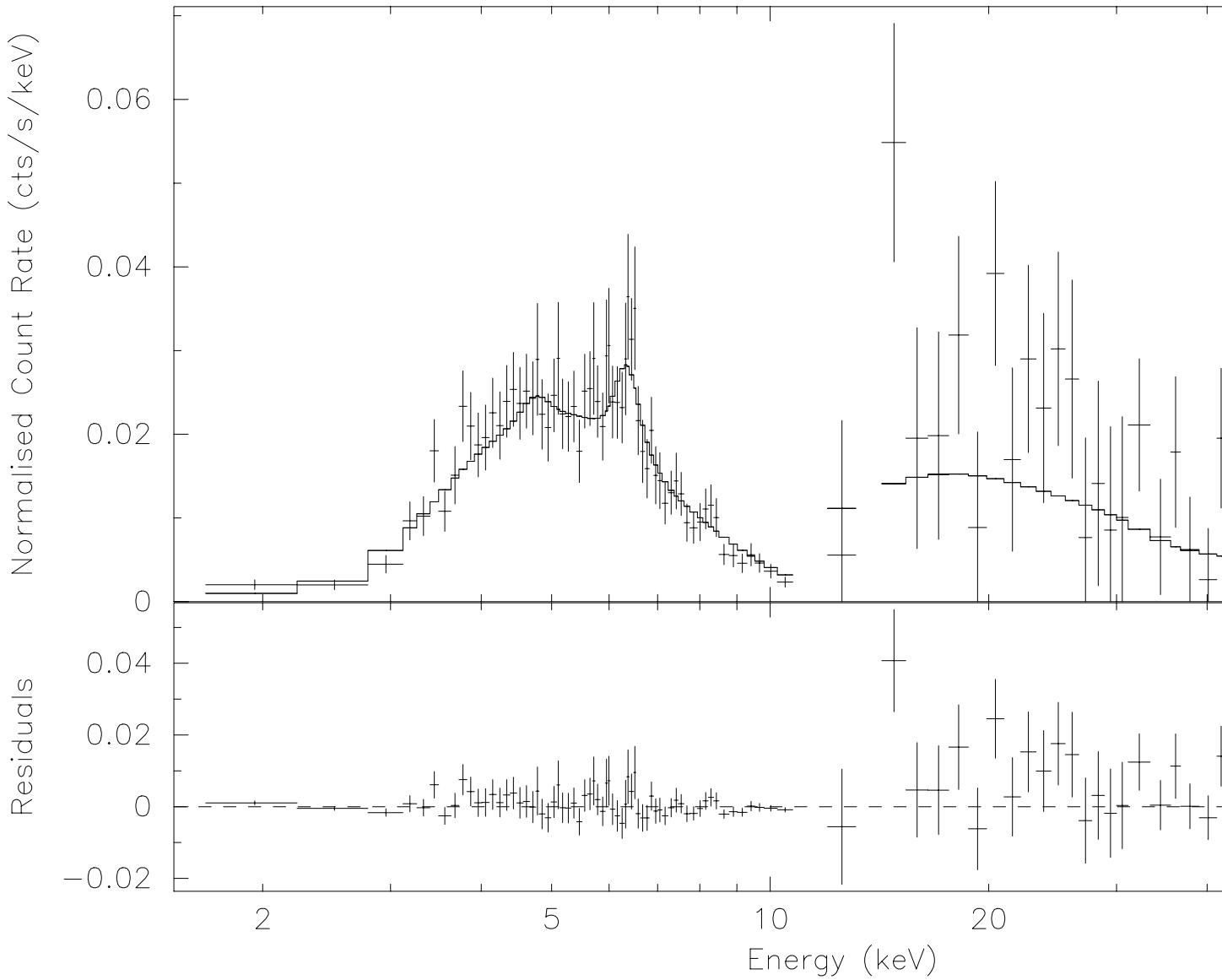

Fig. 4.— Best fitting power law plus gaussian emission line model for the epoch 1997 BeppoSAX-MECS AND PDS data of ESO103-G35 over the energy range 0.6–100 keV (Table 3, fit 5). The figure shows the data and best fit model folded through the instrument response with the residuals in the lower panel.

Table 3: Results of spectral fits to the 1997 dataset[1].

Fits	5	6	7
Model[2]	PL+Gauss[3]	PL+Gauss	PL+Refl+Gauss
N_H ($\times 10^{23}$cm^{-2})	2.02±0.28	$1.68^{+0.23}_{-0.21}$	1.78
F_ν(1 keV)[4]	$0.008^{+0.0078}_{-0.0034}$	$0.003^{+0.002}_{-0.001}$	0.006
α_E	0.9±0.3	$0.49^{+0.19}_{-0.17}$	0.93
Energy (keV)	$6.45^{+0.11}_{-0.19}$	$6.43^{+0.11}_{-0.25}$	6.42
σ (keV)	< 0.3	< 0.4	< 0.4
EW(FeKα)(eV)	250^{+150}_{-110}	260^{+180}_{-110}	193
R (cos i=0.45)			4^{+7}_{-3}
χ^2_ν(dof)	0.66(65)	0.87(96)	0.78(94)
Flux(2-10 keV)[5]	0.95	0.98	0.97

1: All errors are quoted at 90% confidence

2: PL: Power Law; Gauss: Gaussian emission line; Refl: reflection component

3: MECS data only

4: in photons cm^{-2} s^{-1} keV^{-1}

5: in units of 10^{-11} erg cm^{-2} s^{-1}

Table 4: Compilation of spectral parameters for earlier observations of ESO103-G35

Satellite	Instrument	Date	Flux (2-10 keV)[4]	N_H	α_E	Ref[1].	% Error
EXOSAT	ME	247/1983	1.81±0.10	$2.28^{+1.37}_{-.98}$	$0.90^{+0.96}_{-0.34}$	1	90
EXOSAT	ME	110/1984	2.18±0.07	$2.47^{+.81}_{-.65}$	$1.54^{+0.71}_{-0.56}$	1	90
EXOSAT	ME	124/1985	2.46±0.09	$2.37^{+.90}_{-.72}$	$1.23^{+0.78}_{-0.60}$	1	90
EXOSAT	ME	214/1985	2.68±0.18	$0.71^{+.73}_{-.42}$	$0.24^{+0.76}_{-0.31}$	1	90
EXOSAT	ME	225/1985	1.90±0.11	$0.81^{+.54}_{-.39}$	$0.57^{+0.76}_{-0.44}$	1	90
EXOSAT	ME	247/1985	1.22±0.10	$1.67^{+1.95}_{-1.01}$	$1.08^{+1.82}_{-0.54}$	1	90
Ginga	LAC	268/88	2.1±0.7	$1.76^{+0.41}_{-0.31}$	$0.76^{+0.19}_{-0.17}$	2	90[2]
Ginga	LAC	102/91	1.9±0.3	$3.55^{+0.72}_{-0.56}$	$0.84^{+0.08}_{-0.11}$	3	90[3]
ASCA	SIS+GIS	246/94	0.9±0.4	$1.565^{+0.288}_{-0.173}$	$0.37^{+0.33}_{-0.21}$	4	90[3]
ASCA	SIS+GIS	246/94	1.42±0.05[6]	$2.16^{+0.40}_{-0.35}$	$0.89^{+0.35}_{-0.40}$	5	90
ASCA	SIS+GIS	269-270/95	2.36±0.13[6]	$1.68^{+0.54}_{-0.48}$	$0.31^{+0.59}_{-0.57}$	5	90
ASCA	SIS+GIS	078/96	2.38±0.06[6]	$2.16^{+0.26}_{-0.25}$	$1.08^{+0.29}_{-0.28}$	5	90

1: References: 1: Warwick *et al.* 1988, 2: Warwick *et al.* 1993, 3: Smith & Done 1996, 4: Turner *et al.* 1997, 5: Forster *et al.* 1999

2: Average of quoted error on normalization

3: Based upon quoted error in slope

4: In units of 10^{-11} erg cm^{-2} s^{-1}

5: In units of 10^{23} cm^{-2}

6: Errors from photon statistics only

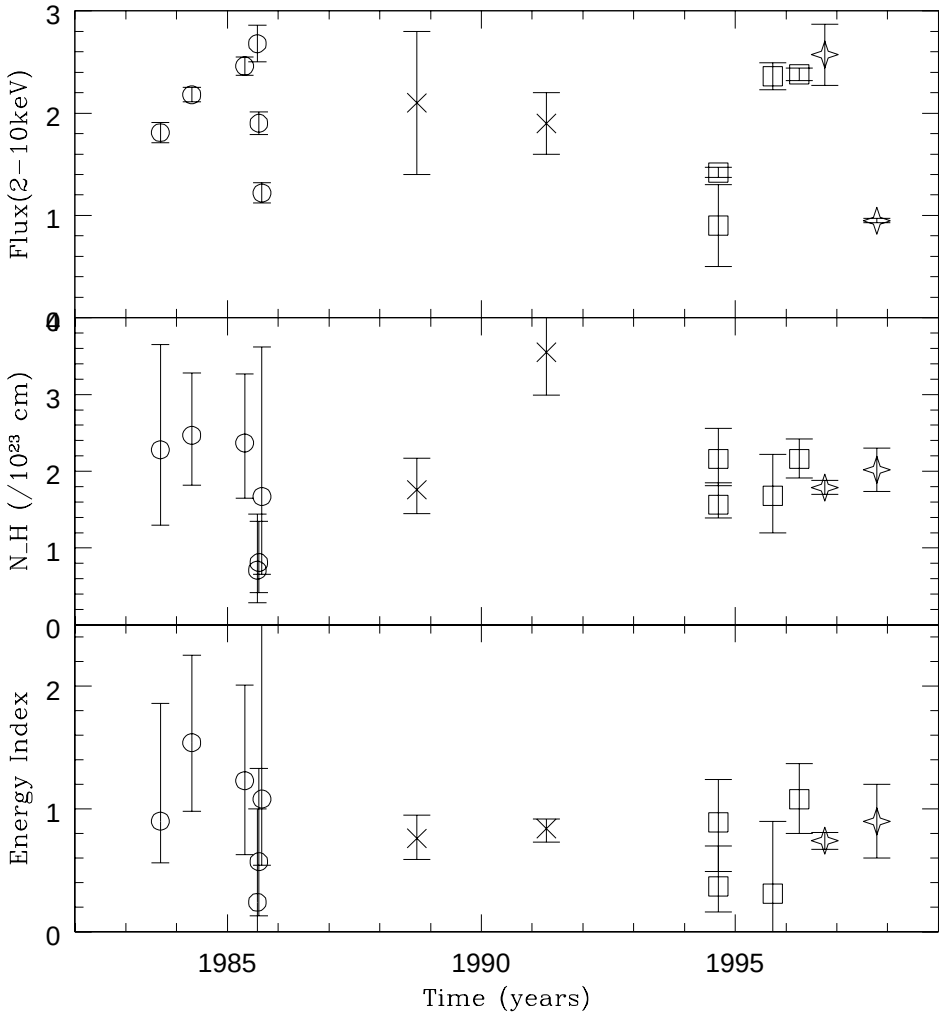

Fig. 5.— Time history of the broad-band (2–10 keV) flux (in units of 10^{-11} erg cm^{-2} s^{-1}), absorbing column density and energy spectral index of ESO103-G35 from 1983−1997. Significant flux variability is present on timescales of a few months while the spectral index remains constant within the errors. The absorbing column has varied on short timescales in the past but in general remains fairly constant as well. The different datasets are indicated as follows: circle: EXOSAT, cross: Ginga, square: ASCA, star: BeppoSAX.

REFERENCES

Antonucci, R.R.J., & Miller, J.S. 1985, ApJ, 297, 621

Arnaud, K. A., 1996, in Jacoby, G. & Barners, J., eds., ADASS V, [ASP, San Francisco]

Awaki, H. 1997, in *Emission Lines in Active Galaxies: New Methods and Techniques*, ed. B.M. Peterson, F.-Z. Cheng & A.S. Wilson, ASP Conf. Series, 113, p 44

Awaki, H., Koyama, K., Inoue, H. & Halpern, J. 1991, PASJ, 43, 195

Braatz, J.A., Wilson, A.S. & Henkel, C., 1997, ApJS, 110, 321

Forster, K., Leighly, K.M. & Kay, P.E. 1999 ApJ, 523, 521

Frontera, F., Dal Fiume, D., Pamini, M., Poulsen, J. M., Basili, A., Franceschini, T., Landini, G., Silvestri, S., Costa, E., Cardini, D., 1991, Advances in Space Research, 11, 281

Gilli, R., Risaliti, G., & Salvati, M., 1999, AA, 347, 424

Gondek, D., Zdziarski, A. A., Johnson, W. N., George, I. M., McNaron-Brown, K., Magdziarz, P., Smith, D. & Gruber, D. E. 1996, MNRAS, 282, 646

Makishima, K., Fujimoto, R., Ishisaki, Y., Kii, T., Loewenstein, M., Mushotzky, R.F., Serlemitsos, P., Sonobe, T., Tashiro, M. & Yaqoob, T. 1994, PASJ, 46, L77

Marshall, F., Boldt, E., Holt, S., Mushotzky, R., Rothschild, R., Serlemitsos, P., Pravdo, S. 1979 ApJS, 40, 657

Matt, G., 1999, in High Energy Processes in Accreting Black Holes, ASP Conference Series 161, ed. J. Poutanen & R. Svensson, p149

Miyoshi, M., Moran, J., Herrnstein, J., Greenhill, L., Nakai, N., Diamond, P., & Inoue, M. 1995, Nature 373, 127

Morris, S.L. & Ward, M.J., 1988, MNRAS, 230, 639

Parmar, A.N., Smith, A. & Bavdaz, M. 1990 in "Observatories in earth orbit and beyond", p457

Phillips, M.M.,Feldman, F.R., Marshall, F.E., Wamstekker, W., 1979, A&A, 76, L14

Piccinotti, G., Mushotzky, R.F., Boldt, E.A., Holt, S.S., Marshall, F.E., Serlemitsos, P.J. & Shafer, R.A., 1982, ApJ, 253, 485

Smith, D.A. & Done, C., 1996, MNRAS, 280, 355

Turner T.J., George, I.M., Nandra, K. & Mushotzky, R.F. 1997, ApJS, 113, 67

Warwick, R. S., Pounds, K. A. & Turner, T. J. 1988, MNRAS, 231, 1145

Warwick, R. S., Sembay, S., Yaqoob, T., Makishima, K., Ohashi, T., Tashiro, M. & Kohmura, Y. 1993, MNRAS, 265, 412

Wilkes, B.J., Schmidt, G.D., Smith, P.S., Mathur, S., McLeod, K.K. 1995, ApJL 455, L13

Yaqoob, T., 2000, in proceedings of the "Large Scale Structure in the X-ray Universe" conference, Santorini, Greece, eds. M. Plionis and I. Georgantopoulos (Editions Frontieres), p. 257